NUCLEAR STRUCTURE CALCULATIONS IN ^{20}Ne WITH NO-CORE CONFIGURATION–INTERACTION MODEL*

Maciej Konieczka, Wojciech Satuła

Faculty of Physics, University of Warsaw
Pasteura 5, 02-093 Warszawa, Poland

(Received December 14, 2016)

Negative parity states in ^{20}Ne and the Gamow–Teller strength distribution for the ground-state beta decay of ^{20}Na are calculated for the very first time using recently developed No-Core Configuration–Interaction model. The approach is based on the multi-reference density functional theory involving isospin and angular-momentum projections. Advantages and shortcomings of the method are briefly discussed.

DOI:10.5506/APhysPolB.48.293

1. Introduction

The single-reference nuclear Density Functional Theory (SR-DFT) is a tool of choice for large-scale calculation of bulk nuclear properties such as masses, radii or quadrupole moments over the entire nuclear chart, see, for example, Ref. [1] and references quoted therein. Despite many incontestable successes, the SR-DFT method has serious drawbacks. It describes nuclei in the intrinsic frame of reference what inevitably leads to spontaneous breaking of fundamental symmetries in the mean-field wave function (Slater determinant). Hence, the method cannot be directly applied to account for structure in a quantum-mechanically rigorous way. Increasing a range of applicability of the nuclear DFT requires, therefore, a restoration of relevant symmetries what can be done by applying projection techniques. It leads, after utilizing the generalized Wick's theorem, to a multi-reference DFT (MR-DFT) having the same form of the energy density functional (EDF) like the underlying SR theory but expressed in terms of transition densities. If the SR-EDF is generated by one of the most popular density-dependent

* Presented at the Zakopane Conference on Nuclear Physics "Extremes of the Nuclear Landscape", Zakopane, Poland, August 28–September 4, 2016.

Skyrme or Gogny forces, the projection leads, however, to singularities in the energy kernels and the entire framework becomes ill defined. Attempts to overcome this difficulty by either directly regularizing the kernels [2, 3] or constructing finite-range regularizable functionals [4] did not bring satisfactory solutions so far. At the moment, the only numerically stable realization of the MR-DFT scheme is possible with the density-independent Skyrme SV [5] or SLyMR0 [6] forces which are *true* interactions. These forces are characterized by anomalously low effective mass which is necessary to obtain a correct saturation property. This, in turn, affects single-particle (s.p.) level density which scales linearly with the inverse of isoscalar effective mass. Whether or not this specific property will affect the spectra and transitions calculated using MR-DFT-rooted approaches is not obvious and is one of the goals of the present study.

The MR-DFT theories can be extended towards no-core configuration–interaction (NCCI) approaches by mixing states projected from the Slater determinants representing (many)particle–(many)hole (or quasiparticle) configurations relevant for a given physical problem. The DFT-rooted NCCI method, hereafter called NCCI for a sake of simplicity, was recently used to compute rotational spectra and electromagnetic transitions in ^{25}Mg [7] and beta-decay matrix elements [8, 9]. The first applications are extremely promising and highly encouraging. Naturally, more systematic studies of NCCI models are needed before trumpeting full success. The aim of this work is to present further tests of the NCCI approach developed recently by our group, see Ref. [9–11]. The model will be applied to calculate negative parity states in ^{20}Ne and the Gamow–Teller strength for the ground-state (g.s.) beta-decay of ^{20}Na.

2. No-Core Configuration–Interaction Model

The MR-DFT approach developed by our group uses a unique combination of the isospin (T) and angular-momentum (I) projections [12]. It provides K- (which is a magnetic quantum number in the intrinsic frame) and T-mixed wave functions projected from arbitrary (many)particle–(many)hole self-consistent mean-field configuration $|\varphi\rangle$

$$|\varphi;\, IM;T_z\rangle^{(j)} = \frac{1}{\sqrt{\mathcal{N}^{(j)}_{\varphi;IM;T_z}}} \sum_K \sum_{T\geq T_z} a^{(j)}_{KT} \hat{P}^T_{T_zT_z} \hat{P}^I_{MK} \,|\varphi\rangle \;, \tag{1}$$

where $\mathcal{N}^{(j)}_{\varphi;IM;T_z}$ is a normalization constant and $\hat{P}^I, \hat{P}^T$ stand for projection operators of a SU(2) group generated by angular-momentum and isospin, respectively. Index j labels different states of given I, M and T_z which are the only conserved quantum numbers.

The configuration space of the NCCI model used hereafter is built in the following way. First, a set of n configurations (Slater determinants) $|\varphi_i\rangle$, $i = 1, 2, \ldots, n$ is calculated self-consistently using the Hartree–Fock (HF) method with the $\mathrm{SV_{SO}}$ force which is a variant of the SV parametrization with the strength of the spin-orbit term increased by 20%, see Ref. [9]. In the set, we include the g.s. and low-lying particle–hole (p–h) excitations of a given parity and signature as these symmetries are conserved at the HF stage of our calculations. Thus, both the aligned ($|h\rangle \otimes |\tilde{p}\rangle$ or $|\tilde{h}\rangle \otimes |p\rangle$) and antialigned ($|h\rangle \otimes |p\rangle$ or $|\tilde{h}\rangle \otimes |\tilde{p}\rangle$) p–h excitations are taken into account. Moreover, in the $N = Z$ nuclei, due to the symmetrization caused by isospin projection, we limit ourselves to neutron p–h configurations. It means that, in the case of ^{20}Ne, the total number of linearly-independent positive parity p–h configurations covering the *sd* shell is equal to ten. Let us underline that our p–h configurations involve excitation among deformed Nilsson states, see Fig. 1, which are mixtures of many (multi)particle–(multi)hole spherical shell-model (SM) configurations.

Eventually, the states $|\varphi_i; IM; T_z\rangle^{(j)}$ are mixed. At this stage, we solve the Hill–Wheeler equation using the same $\mathrm{SV_{SO}}$ Skyrme interaction (plus Coulomb) in order to obtain the eigenenergies and the associated eigenfunctions

$$E^{(k)}_{IM;T_z} \quad \text{and} \quad |IM;T_z\rangle^{(k)} = \frac{1}{\sqrt{\mathcal{N}^{(k)}_{IM;T_z}}} \sum_{ij} c^{(k)}_{ij} \, |\varphi_i; IM; T_z\rangle^{(j)} \, . \qquad (2)$$

For further details, we refer reader to Ref. [11] .

3. Numerical results in ^{20}Ne

3.1. Cross-shell excitations and negative parity states

The DFT-rooted NCCI approach is, by construction, capable to describe both the positive and negative parity states using single universal two-body interaction. It takes into account core-polarization or deformation effects inheriting them from the underlying mean-field treatment. This is of paramount importance for investigating cross-shell excitations to the intruder or high-j orbits which polarize or often statically deform a nucleus.

An example of such calculations involving cross-shell p–h excitations in ^{20}Ne is shown in Fig. 1. In this preliminary calculations, we limited the NCCI configuration space to two negative parity p–h configurations (see the right panel Fig. 1), which correspond to aligned and antialigned excitations from the negative parity Nilsson level [101]3/2 to the lowest available positive parity Nilsson level [211]3/2, see the left part of Fig. 1. The g.s. is correlated

over the entire positive-parity subspace described in Subsect. 3.2. Comparison between the calculated negative parity states and the data shows that we systematically overestimate the excitation energy of the negative-parity states by ~ 3 MeV. The primary reason can be traced back to a large, ~ 10 MeV, energy splitting between the [101]3/2 and [211]3/2 Nilsson levels in the g.s. configuration. The polarization effect (or an increase of deformation) that accompany the p–h excitation reduces this energy by ~ 2 MeV but the effect is too small to account for experimental data. Note however, that the order and the spacing of the calculated negative parity states is in surprisingly good agreement with the data except for the 1^- states. It remains to be studied how this picture would evolve in function of a number of negative parity configurations.

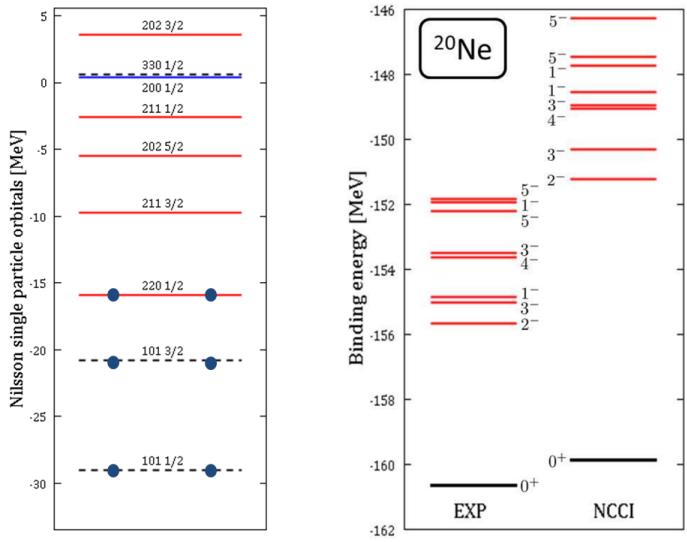

Fig. 1. (Color online) Left part shows a subset of neutron s.p. levels in the g.s. of ^{20}Ne relevant for this work. The orbitals are labelled with approximate Nilsson quantum numbers. Dots indicate occupied levels. Right part shows the calculated spectrum of negative-parity states in ^{20}Ne in absolute energy scale. See the text for further details.

3.2. Gamow–Teller strength distribution

Recently, we performed the first systematic study of the g.s. Gamow–Teller (GT) matrix elements in $T = 1/2$ mirror nuclei using DFT-rooted models [9]. It was shown that the MR-DFT calculations involving only one configuration representing the g.s. provides very accurate description of the matrix elements and that the results are stable against mixing additional

configurations. However, in order to account for transitions to the excited states, especially to the configurations involving particles occupying close-lying s.p. levels, the mixing through the NCCI is indispensable.

In this section, we perform the calculation of GT strength function for the g.s. decay of ^{20}Na. The $I = 2^+$ g.s. of ^{20}Na was calculated using the NCCI model involving four lowest-lying p–h configurations. The distribution of $I = 1^+, 2^+$ and 3^+ states in the daughter nucleus ^{20}Ne was computed using the g.s. and 10 p–h configurations. All configurations are axially-deformed. The g.s. corresponds to $\beta_2 = 0.42$, while the excited states have $\beta_2 \in (0.2; 0.3)$. The calculated spectra of $0^+, 1^+, 2^+$, and 3^+ excited states are systematically too low in energy by ~ 2 MeV. This deficiency impacts the GT strength function which is presented in Fig. 2 in comparison with the USDb SM results of Ref. [13] and experimental data. The NCCI strength distribution is also shifted towards lower energies with respect to both the SM calculations and experimental data. In particular, the resonant pick is shifted by ~ 3 MeV. Microscopically, the GT strength distribution is very sensitive to the positions of specific s.p. Nilsson levels in a potential well. Thus, it may serve as an excellent tool to attempt to identify the correct order and spacing of orbitals in a given nucleus. It seems that the s.p. structure and in turn the GT strength distribution can be improved by increasing the spin-orbit strength. Local optimization of the interaction is, however, beyond the scope of this work.

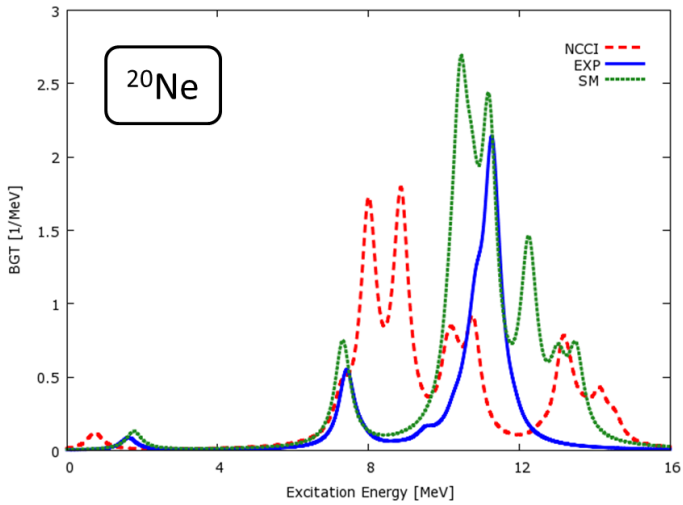

Fig. 2. (Color online) Gamow–Teller strength function in ^{20}Ne smeared by means of the Lorentz function of half-width of 0.5 MeV. Solid line labels experimental data. The SM calculations of Ref. [13] are depicted by dotted line. Dashed line marks the DFT-rooted NCCI results.

4. Summary and outlook

We presented very preliminary results of the DFT-rooted NCCI calculations for negative-parity states in ^{20}Ne and the GT strength for g.s. decay of ^{20}Na. It is shown that general features of experimental data can be captured with relatively limited number of p–h configurations. We encountered problems in reproducing the excitation energy of the first 2^- state or the position of resonant picks in the GT distribution. These quantities are very sensitive to the positions of s.p. levels in the mean-field potential well. Preliminary results indicate that an increase in the strength of spin-orbit interaction may considerably improve the results.

This work was supported by the Polish National Science Center (NCN) under contract No. 2014/15/N/ST2/03454. We acknowledge the CIS-IT National Centre for Nuclear Research (NCBJ), Poland and CSC-IT Center for Science Ltd, Finland for allocation of computational resources.

REFERENCES

[1] J. Erler *et al.*, *Nature* **486**, 509 (2012).
[2] M. Bender, T. Duguet, D. Lacroix, *Phys. Rev. C* **79**, 044319 (2009).
[3] W. Satuła, J. Dobaczewski, *Phys. Rev. C* **90**, 054303 (2014).
[4] F. Raimondi, K. Bennaceur, J. Dobaczewski, *J. Phys. G: Nucl. Part. Phys.* **41**, 055112 (2014).
[5] M. Beiner, H. Flocard, N. Van Giai, P. Quentin, *Nucl. Phys. A* **238**, 29 (1975).
[6] J. Sadoudi, T. Duguet, J. Meyer, M. Bender, *Phys. Rev. C* **88**, 064326 (2013).
[7] B. Bally, B. Avez, M. Bender, P.-H. Heenen, *Phys. Rev. Lett.* **113**, 162501 (2014).
[8] W. Satuła, J. Dobaczewski, M. Konieczka, W. Nazarewicz, *Acta Phys. Pol. B* **45**, 167 (2014).
[9] M. Konieczka, P. Bączyk, W. Satuła, *Phys. Rev. C* **93**, 042501(R) (2016).
[10] W. Satuła, J. Dobaczewski, M. Konieczka, *JPS Conf. Proc.* **6**, 020015 (2015).
[11] W. Satuła, P. Bączyk, J. Dobaczewski, M. Konieczka, *Phys. Rev. C* **94**, 024306 (2016).
[12] W. Satuła, J. Dobaczewski, W. Nazarewicz, T.R. Werner, *Phys. Rev. C* **86**, 054316 (2012).
[13] B.A. Brown, B.H. Wildenthal, *At. Data Nucl. Data Tables* **33**, 347 (1985).